Quaternary Science Reviews 334 (2024) 108715

Contents lists available at ScienceDirect

Quaternary Science Reviews

journal homepage: www.elsevier.com/locate/quascirev

Comparisons of interglacial vegetation responses to climate variability between the Massif Central, France, and the Balkan Peninsula since 423 ka

Patrick Schläfli[a,b,c,*], Erika Gobet[b,c], Jacques-Louis de Beaulieu[d], Maurice Reille[d], Hendrik Vogel[a,c], Fritz Schlunegger[a], Willy Tinner[b,c]

[a] *Institute of Geological Sciences, University of Bern, Switzerland*
[b] *Institute of Plant Sciences, University of Bern, Switzerland*
[c] *Oeschger Centre for Climate Change Research, University of Bern, Switzerland*
[d] *IMBE-UMR CNRS 7263/IRD 237/Aix-Marseille Université, Europôle Méditerranéen de l'Arbois, BP 80, 13545, Aix-en-Provence, Cedex 04, France*

ARTICLE INFO

Handling Editor: Dr Donatella Magri

Keywords:
Middle and Late Pleistocene
Velay long sequence
Lake Ohrid
Age-depth model
Climate forcing

ABSTRACT

Palynological long sequences offer a unique possibility to study the effect of pronounced climate change on vegetation dynamics over several glacial-interglacial cycles. Such long sequences are rare, especially outside of the Mediterranean realm. Additionally, they often lack robust chronologies, which are a precondition for comparisons across records and proxies. In this study we present a refined chronology of the Velay pollen sequence (0–423 ka) from south-central France by tuning it to the recently published Lake Ohrid pollen sequence from the southern Balkans, which itself has a vegetation-independent, numerical chronology. Furthermore, we use ordination techniques in combination with independent palaeo-temperature proxies and seasonality as explanatory variables for both sites. This allows us to infer climatic responses of interglacial vegetation over a broad ecological gradient, i.e., from a cool-temperate to a submediterranean site. Our analysis shows that temperature is a significant determinant for interglacial vegetation composition at both sites but explains slightly more variance at cool-temperate Velay compared to submediterranean Lake Ohrid, where precessional-driven moisture availability might have had a greater influence. Temperate oceanic taxa such as *Abies* and *Taxus* were most affected by comparably cool or warm interglacials at Velay, whereas at Lake Ohrid, the same accounts for Mediterranean taxa such as *Quercus ilex*, *Q. cerris*, or *Ostrya/Carpinus orientalis*. Responses of single taxa and vegetation groups to seasonality changes over the last five interglacials suggest that species-specific niche preferences have remained stable since 423 ka. Additionally, we suggest that unless a future climate exceeds the MIS 5e anomaly of c. +1.3 °C (if compared to the Holocene), evergreen Mediterranean taxa such as *Quercus ilex* will not expand into temperate biomes north of the Alps. However, even temperature rises below +1.3 °C will cause a restructuring of the current vegetation in both areas.

1. Introduction

Palynological vegetation reconstructions from long sedimentary sequences (i.e., spanning several glacial-interglacial cycles) are key records for understanding the complex interactions between climate and the environment (e.g., Herzschuh et al., 2016). Although such archives are rare in Europe, several terrestrial long sequences have been described so far, e.g., those from Tenaghi Philippon (Wijmstra, 1969; Wijmstra and Smit, 1976; van der Wiel and Wijmstra, 1987a, 1987b; Koutsodendris et al., 2023), Ioannina (Tzedakis, 1993, 1994; Tzedakis et al., 2003; Roucoux et al., 2008, 2011), Lake Ohrid (Sadori et al., 2016; Donders et al., 2021), Valle di Castiglione (Follieri et al., 1988) in Southern Europe, and Velay (Reille et al., 2000; Beaulieu et al., 2001) and Rodderberg (Zolitschka et al., 2014; Schläfli et al., 2023) in Western and Central Europe, respectively (Fig. 1). Additionally, palynological studies have been carried out on marine long sequences from the Iberian margin (Desprat et al., 2005, 2006, 2007, 2009; Sanchez Goñi et al., 2018) (a and b in Fig. 1). To fully exploit their potential for exploring e.g., similarities or dissimilarities in major land cover changes, climate-environment interactions, refugia and migration dynamics, numerical age-depth models are crucial, and the establishment of such models has unfortunately still been a major difficulty. Although dating

---

* Corresponding author. Institute of Geological Sciences, University of Bern, Switzerland.
E-mail address: patrick.schlaefli@unibe.ch (P. Schläfli).

https://doi.org/10.1016/j.quascirev.2024.108715
Received 30 October 2023; Received in revised form 6 May 2024; Accepted 6 May 2024

techniques have improved over the last decades and already contributed substantially to our knowledge about past environmental changes (Geyh and Müller, 2005; Lamothe, 2016), their applicability is often restricted to specific materials and time scales (Lian and Roberts, 2006). Moreover, error estimates are often beyond the required accuracy and precision for a comparison of climate and environmental data. A further dating approach is offered by pollen-biostratigraphy, which has proven useful for e.g., correlating interglacial and interstadial records (Bittmann, 1992; Beaulieu et al., 2001; Schläfli et al., 2021, 2023). However, biostratigraphic methods often result in relative ages and are hence not ideal as a primary dating method if absolute ages are required.

Past interglacial climates have increasingly been the focus of recent research (e.g., Tzedakis et al., 2009; Past Interglacials Working Group of PAGES, 2016; Tzedakis et al., 2017). As Birks (2019) pointed out, “A major challenge is to integrate these advances into interpretations of pollen-stratigraphical patterns between different interglacials“. In this paper, we use the recently published Lake Ohrid pollen record (Donders et al., 2021) as tuning target and thus as reference to establish a new age-depth model for the long sequence from Velay (Reille et al., 2000; Beaulieu et al., 2001). The palynological record of Lake Ohrid is most suited for this purpose due to its robust and vegetation-independent chronology (Francke et al., 2016; Zanchetta et al., 2016; Wagner et al., 2017, 2019). The previous age-depth model of the Velay record was established by correlating the Velay composite profile with the marine SPECMAP curve (Imbrie et al., 1984) using glacial-to-deglacial transitions as tie points (Tzedakis et al., 1997). However, more recent pollen data (Reille et al., 2000) were not included for establishing this previous chronology. Here we combine the currently available pollen data from the Velay and Ohrid records in an effort to reconstruct a common chronology. This approach allows us to statistically compare the pollen-inferred vegetation dynamics at the two sites with independent climate proxy data (e.g., benthic $\delta^{18}O$ as temperature proxy) to assess the ecosystem responses. Accordingly, the aim of this contribution is to (i) assign a new chronology to the palynologically updated Velay record, (ii) numerically characterize different interglacial phases in terms of vegetation types, and to (iii) quantify the importance of interglacial climate forcing by linking the pollen data with vegetation-independent proxy data. The ultimate goal is to compare the ecosystem response dynamics to climate forcing at both sites. We hypothesize that temperature is the main driver of vegetational changes over orbital timescales in both bioclimatic regions (i.e., cool-temperate and submediterranean).

2. Datasets and methods

2.1. Site descriptions and available data

Lake Ohrid, at the border between Albania and North-Macedonia, is located at the transition from the Mediterranean to the Alpine biogeographic regions (European Environment Agency, 2016; Sinopoli et al., 2018) (Fig. 1). The DEEP core from Lake Ohrid (41°02′57″N, 20°42′54″E; 693.5 m a.s.l.) covers the last 1.36 Ma and is hence one of the longest terrestrial environmental archives in Europe (Wagner et al., 2023). Its chronological framework is based on dates from 54 tephra layers, palaeomagnetic reversals, and orbital tuning of biogeochemical proxies (Francke et al., 2016; Zanchetta et al., 2016; Wagner et al., 2017, 2019). Pollen-based environmental reconstructions spanning multiple glacial-interglacial cycles have previously been published by Sadori et al. (2016) and Donders et al. (2021). Mean annual precipitation at Ohrid meteorological station (760 m a.s.l.), located close to the lake shore, is 662 mm with maxima in winter and minima in summer. Mean January and July temperatures are 2.4 °C and 20.8 °C, respectively

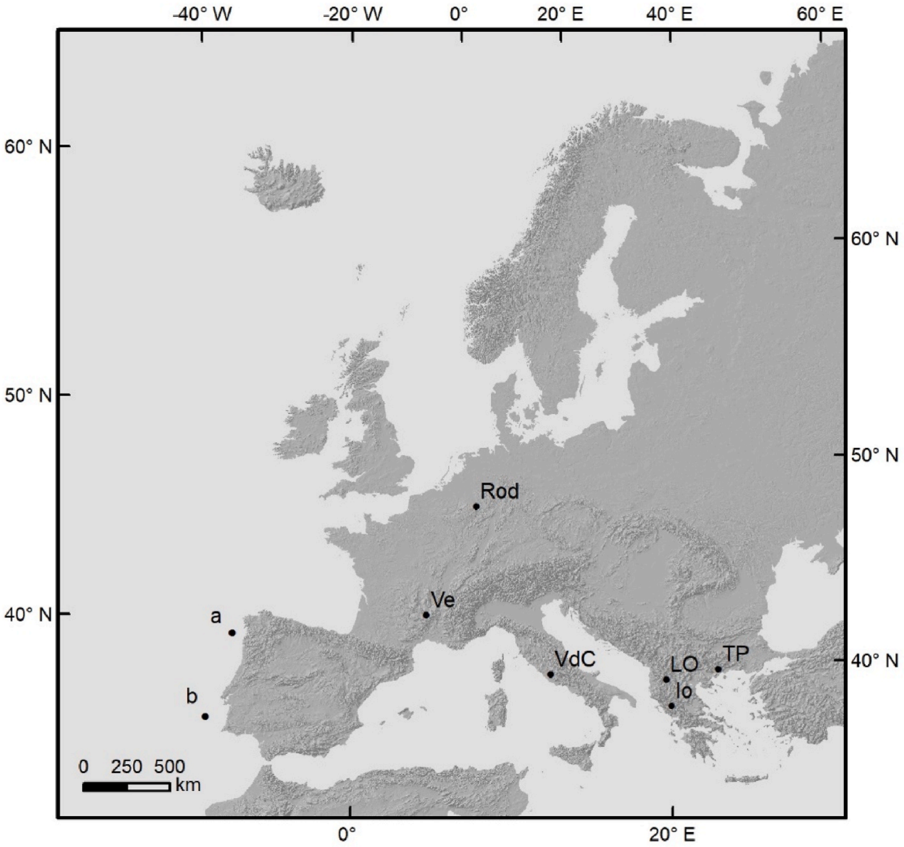

Fig. 1. Map of Europe showing the terrestrial and marine sites mentioned in the text. The record of Velay (Ve) consists of the three sites Ribains, Lac du Bouchet, and Praclaux (see text for details). a = MD95-2042, MD01-2443, and IODP U1385, b = MD99-2331, MD01-2447, and MD03-2697, Rod = Rodderberg, VdC=Valle di Castiglione, LO=Lake Ohrid, Io = Ioannina, TP=Tenaghi Philippon. For references the reader is referred to the main text.

(period 1971–2000; WMO, 2022). The climate with dry and warm summers is cool-temperate (Csb) close to the transition to warm-temperate (Csa) conditions; Kottek et al. (2006). At the lowest elevations in the catchment the modern submediterranean vegetation consists of deciduous and semi-deciduous oaks (*Quercus cerris*, *Q. trojana*, *Q. pubescens*, *Q. frainetto*), hop-hornbeam (*Ostrya carpinifolia*), manna ash (*Fraxinus ornus)* and oriental hornbeam (*Carpinus orientalis*). Oromediterranean mesophilous forests with mostly beech (*Fagus sylvatica*) and hornbeam (*Carpinus betulus*) grow at higher elevations, followed by mixed silver fir (*Abies alba*) and Bulgarian fir (*Abies borisii-regis*) forests at the transition to grassland vegetation with *Juniperus excelsa* (Matevski et al., 2011; Sadori et al., 2016; Sinopoli et al., 2018; Donders et al., 2021; Brechbühl et al., 2023).

The Velay record from the Massif Central, France, is the only long sequence in Europe outside of the Mediterranean region, which covers five interglacials (the Holocene included) including an uninterrupted record to the present (Fig. 1). The previously published composite profile (Reille et al., 2000; Beaulieu et al., 2001) is based on drill cores from the sites Praclaux (44°49′N, 3°50′E; 1000 m a.s.l.), Lac du Bouchet (44°55′N, 3°47′E; 1200 m a.s.l.), and Ribains (44°50′09″N, 3°49′16″E; 1080 m a.s.l.). At Le Puy-Loudes meteorological station (833 m a.s.l.) c. 20 km north of the study site, mean annual precipitation is 682 mm, and mean January and July mean temperatures are 1.4 °C and 17.7 °C, respectively (period 1991–2020; Météo France, 2022). Because the study site is situated at 1000–1200 m a.s.l. and thus higher than the Le Puy-Loudes station, the mean temperatures might be around 1–2 °C lower at the site. The climate is classified as cool-temperate oceanic with warm summers (Cfb; Kottek et al., 2006). Compared to Lake Ohrid, the climate at Velay is c. 3–5 °C cooler. In addition, maximum temperature differences between the two sites occur during summer. The current vegetation surrounding the Velay site consists of meadows, the heath shrubs Scotch broom (*Cytisus scoparius*) and Pyrenean broom (*Cytisus purgans*). Today's Scots pine (*Pinus sylvestris*) woodlands in the area have been managed in recent times (Beaulieu and Reille, 1992; Reille et al., 2000) in the montane belt, where by nature beech (*Fagus sylvatica*) forests would be important (Beaulieu et al., 1984). More thermophilous *Quercus robur*, *Q. petraea*, and *Castanea sativa* grow at elevations below the site (Beaulieu and Reille, 1992).

Table 1
Time periods covered by the different Velay sequences in the presented composite profile.

sequence	site	time period	original publication
B5	Lac du Bouchet	0–12 ka	Reille and Beaulieu (1988)
D	Lac du Bouchet	12–111 ka	Reille and Beaulieu (1990)
Ribains	Ribains	111–138 ka	Beaulieu et al. (1984)
H	Lac du Bouchet	138–206 ka	Reille et al. (1998)
I	Lac du Bouchet	206–218 ka	Reille et al. (1998)
H	Lac du Bouchet	218–322 ka	Reille et al. (1998)
PraC	Praclaux	322–423 ka	Reille et al. (2000)

2.2. *New composite profile and age-depth model of the long sequence from Velay*

The previous age-depth model was established by correlating the Velay composite profile with the marine SPECMAP curve (Imbrie et al., 1984) using glacial-to-deglacial transitions as tie points (Tzedakis et al., 1997). For the oldest part (287–430 ka) of the composite profile, pollen data of the core Pra 1995 (Reille and Beaulieu, 1995) that was drilled at Praclaux was used. Since then, a further drilling at the Praclaux site (PraC) yielded a more complete sedimentary sequence (Reille et al., 2000). For this study, we updated the available information to generate a new composite profile consisting of the sequences B5, D, I and H from the Lac du Bouchet site, the latest sequence PraC from the Praclaux site, and Ribains from the Ribains site (Table 1). The Bouchet 2 interstadial is incomplete in sequence H. For this reason, we exchanged pollen zones H 16, H 17, and H 18 with pollen zones I 3a to I 7 of sequence I (according to the correlation table in Reille et al., 1998).

We use the arboreal pollen excluding *Pinus* (AP-*Pinus*) signal of the latest long sequence from Lake Ohrid (Donders et al., 2021) as tuning target (Fig. 2). Following the original approach of Tzedakis et al. (1997), we excluded *Pinus* from the terrestrial pollen sum of the Velay composite profile. To determine tie points (n = 19), we used visual criteria, i.e., the onset of the steep increase (rational pollen limit; see Lang et al., 2023) and decrease of AP-*Pinus* at the beginning and the end of interglacials/interstadials. We thus follow the biostratigraphic framework as previously defined in the original publications (Beaulieu et al., 2001; Donders et al., 2021). In cases where the AP-*Pinus* abundances do not allow to unambiguously delimit interglacials/interstadials, i.e., at the end of MIS 7c and MIS 11c as well as at the beginning of MIS 7a and MIS 11a, no tie points were set (Fig. 2). In a next step, the ages from the Lake Ohrid chronology were transferred to the Velay composite profile at the tie points. Between two tie points, the ages were linearly interpolated. The chronology of the youngest part (0–12 ka, including the tie point at the onset of the Holocene) is based on calibrated ^{14}C ages from the sequence B5, which were taken from the European Pollen Database (EPD).

2.3. *Processing the Velay and Lake Ohrid pollen data*

We pooled and linearly interpolated the pollen data of both sites to a 1 ka resolution in order to fit the resolution of the climate proxy data, which are described in detail in the next chapter. Additionally, we

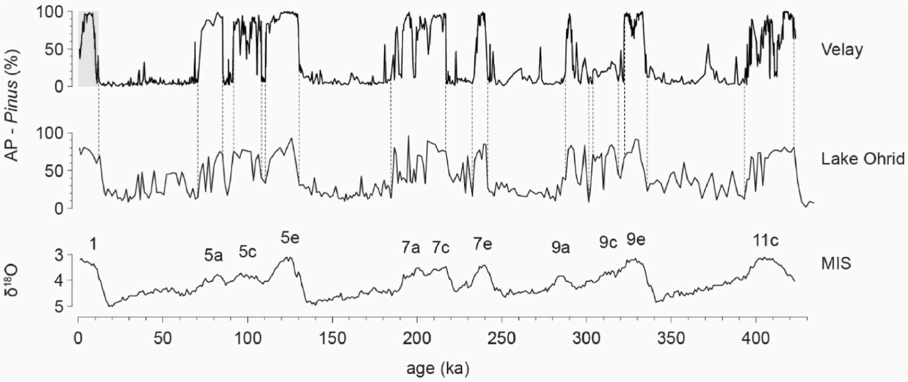

Fig. 2. Illustration of tie points (dotted vertical lines) used to tune the percentages of arboreal pollen excluding *Pinus* (AP - *Pinus*) of the Velay composite (top) to the Lake Ohrid record (middle; Donders et al., 2021). The chronology between 0 ka and the youngest tie point at 12.125 ka (grey bar) is based on calibrated radiocarbon dates of the BOUCH B5 drill core. For selection criteria of the tie points the reader is referred to the methods section of this paper. Bottom: Marine isotope stages (MIS; Lisiecki and Raymo, 2005) with interglacial and interstadial substages relevant for the text.

Table 2
Vegetation types and included pollen taxa for Velay and Lake Ohrid.

Vegetation type	included taxa Velay	included taxa Lake Ohrid
steppic	*Artemisia*, Asteroideae, Caryophyllaceae, Chenopodiaceae, Cyperaceae, *Dryas*, *Ephedra*, Poaceae	*Artemisia*, Asteroideae, Caryophyllaceae, Chenopodiaceae, Cyperaceae, *Ephedra distachya* type, *Ephedra fragilis* type, Poaceae
boreal	*Betula*, *Hippophae*, *Juniperus*, *Picea*, *Pinus*	*Betula*, *Hippophae*, Cupressaceae (mostly *Juniperus*), *Larix*, *Picea*, *Pinus*
temperate continental	*Acer*, *Corylus*, *Fraxinus*, deciduous *Quercus*, *Tilia*, *Ulmus*	*Acer*, *Corylus*, *Fraxinus excelsior/oxycarpa*, *Quercus robur* type, *Tilia*, *Ulmus*
temperate oceanic	*Abies*, *Buxus*, *Carpinus*, *Castanea*, *Fagus*, *Hedera*, *Ilex*, *Taxus*, *Viburnum*, *Vitis*	*Abies*, *Buxus*, *Carpinus*, *Castanea*, *Fagus*, *Hedera*, *Ilex*, *Viburnum*, *Vitis*
Mediterranean	Oleaceae, *Phillyrea*, *Pistacia*, *Quercus ilex*	*Arbutus*, Arecaceae, *Ceratonia*, *Cistus*, *Diospyros*, *Fraxinus ornus*, *Myrtus*, *Ostrya/Carpinus orientalis*, *Olea/Phillyrea*, *Pistacia*, *Quercus ilex*, *Quercus cerris* type
wetland	*Alnus*, *Platanus*, *Populus*, *Salix*	*Alnus*, *Platanus*, *Populus*, *Salix*, *Tamarix*, *Taxodium* type

grouped the pollen taxa into 6 vegetation types: steppic, boreal, temperate continental, temperate oceanic, Mediterranean, and wetland (Table 2). This categorization was accomplished through considering the climate and habitat requirements of the plant species behind the pollen types (i.e., their today's niche, autecology and occurrence in the biomes of Europe, see Böhling et al., 2002; Pignatti, 2005; Ellenberg, 2009; Lang et al., 2023) and allowed us to identify the impact of climate changes on specific vegetation types.

The Lake Ohrid record has so far been divided into interglacial and glacial local pollen superzones (LPSZ; Sadori et al., 2016; Donders et al., 2021). For our scope we established a more detailed subzonation considering interstadials and stadials as well. This was accomplished by using AP-*Pinus* = 70 % as boundary between interglacials, stadials and interstadials within interglacial LPSZ. We named the resulting subzones according to the nomenclature of marine isotope substages with the letters a–e (Table 3) following the approach of Railsback et al. (2015).

2.4. Statistical analyses

To identify interglacial-specific vegetation assemblages and responses to climate, we applied a Redundancy Analysis (RDA) in Canoco 5.10 (ter Braak and Šmilauer, 2018) on the pooled and interpolated datasets of both sites. The choice of a linear method (RDA) is justified by the gradient lengths of both datasets (Velay: 2.2 SD; Lake Ohrid: 1.4 SD). Prior to the RDA, the data was log-transformed. We ran a permutation test (999 permutations) implemented in Canoco 5.10 to assess the Bonferroni-corrected (Shaffer, 1995) significance of all axes and explanatory variables. For the latter of which we used the global benthic $\delta^{18}O$ (LR04; Lisiecki and Raymo, 2005) and the global average surface temperature (GAST; Snyder, 2016) stacks. The two variables integrate globally distributed benthic $\delta^{18}O$ records or sea surface temperature (SST) reconstructions (Mg/Ca ratios of planktonic foraminifera, transfer functions with species assemblages, alkenone indices), respectively, at a 1 ka resolution. By only considering marine reconstructions, GAST neglects the amplification of temperature changes on the continents compared to the oceans. However, this does not affect our comparison of vegetational responses between specific interglacials, assuming that the temperature discrepancy between land and sea was constant through time. Dating uncertainties and uncertainties from proxy reconstructions at individual sites used for the stack may affect GAST (Snyder, 2016). Nevertheless, the close relation of GAST with the benthic $\delta^{18}O$ (Lisiecki and Raymo, 2005), Antarctica temperatures (Parrenin et al., 2013) and atmospheric GHG concentrations (Bereiter et al., 2015), underlines the robustness of GAST (Snyder, 2016) and its suitability as explanatory variable in our RDA. As an additional explanatory variable, we used the insolation difference between June and December solstice (seasonal insolation difference) at 65°N. The related values were calculated with the R-package *palinsol* (Crucifix, 2016) using the la04 solution (Laskar et al., 2004). This allowed quantifying and comparing the variance explained by the climate proxies between both sites. For a comparison of the data recording interglacial conditions, we grouped those interglacial samples that represent the climate optimum phases (AP>80 % for Velay; AP>70 % for Lake Ohrid) into polygons. Response curves are frequently used to model the behavior of species to changes in environmental drivers. We calculated response curves of (i) vegetation types and (ii) selected pollen taxa (major forest constituents) to changes in seasonality (seasonal insolation difference) during all interglacials since 423 ka. To do so, we fitted Generalized Additive Models (GAM; Hastie and Tibshirani, 1999) to pollen percentages of interglacial samples and the corresponding insolation data. As for the RDA, this was accomplished using the Canoco 5.10 software.

3. Results and interpretations

3.1. Comparison of the old and new age-depth models

Our tuning approach differs from that previously published by Tzedakis et al. (1997). In particular, we used 8 additional tie points compared to the original approach, in which no tie points were set at the end of interglacials and interstadials (i.e., at deglacial-to-glacial transitions). The reason for the procedure selected by Tzedakis et al. (1997) was that the terrestrial and marine boundaries at the end of interglacials and interstadials are likely to be diachronous (Tzedakis et al., 1997;

Table 3
Correlation of Lake Ohrid superzones (LPSZ) and subzones with Velay warm stages and marine isotope stages (MIS).

Lake Ohrid LPSZ (Sadori et al., 2016; Donders et al., 2021)	Lake Ohrid subzones	Velay composite (Reille et al., 2000; Beaulieu et al., 2001)	MIS
OD-1	OD-1	Holocene	1
OD-3	OD-3a	St. Geneys 2	5a
	OD-3c	St. Geneys 1	5c
	OD-3e	Ribains	5e
OD-6	OD-6a	Bouchet 3	7a
	OD-6c	Bouchet 2	7c
	OD-6e	Bouchet 1	7e
OD-8	OD 8a	Amargiers	9a
	OD-8c	Ussel	9c
	OD-8e	Landos	9e
OD-10	N.A.	Jagonas 2 Jagonas 1	11a (?)
	OD-10c	Praclaux	11c

N.A. = not assigned in case the biostratigraphic boundaries are ambiguous.

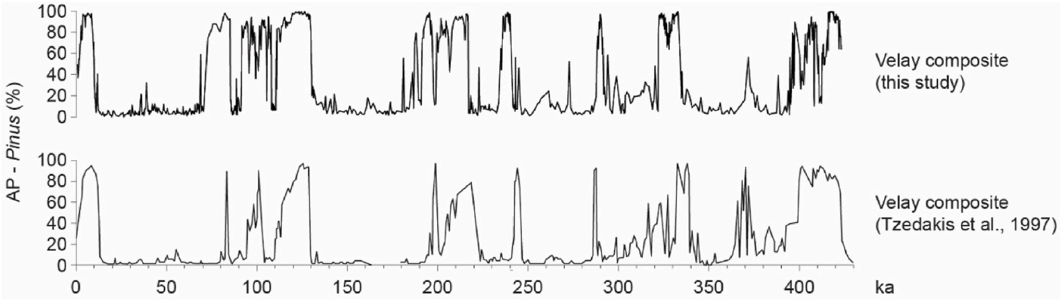

Fig. 3. Comparison of age-depth models for the Velay composite profile. Top: this study, bottom: redrawn after Tzedakis et al. (1997).

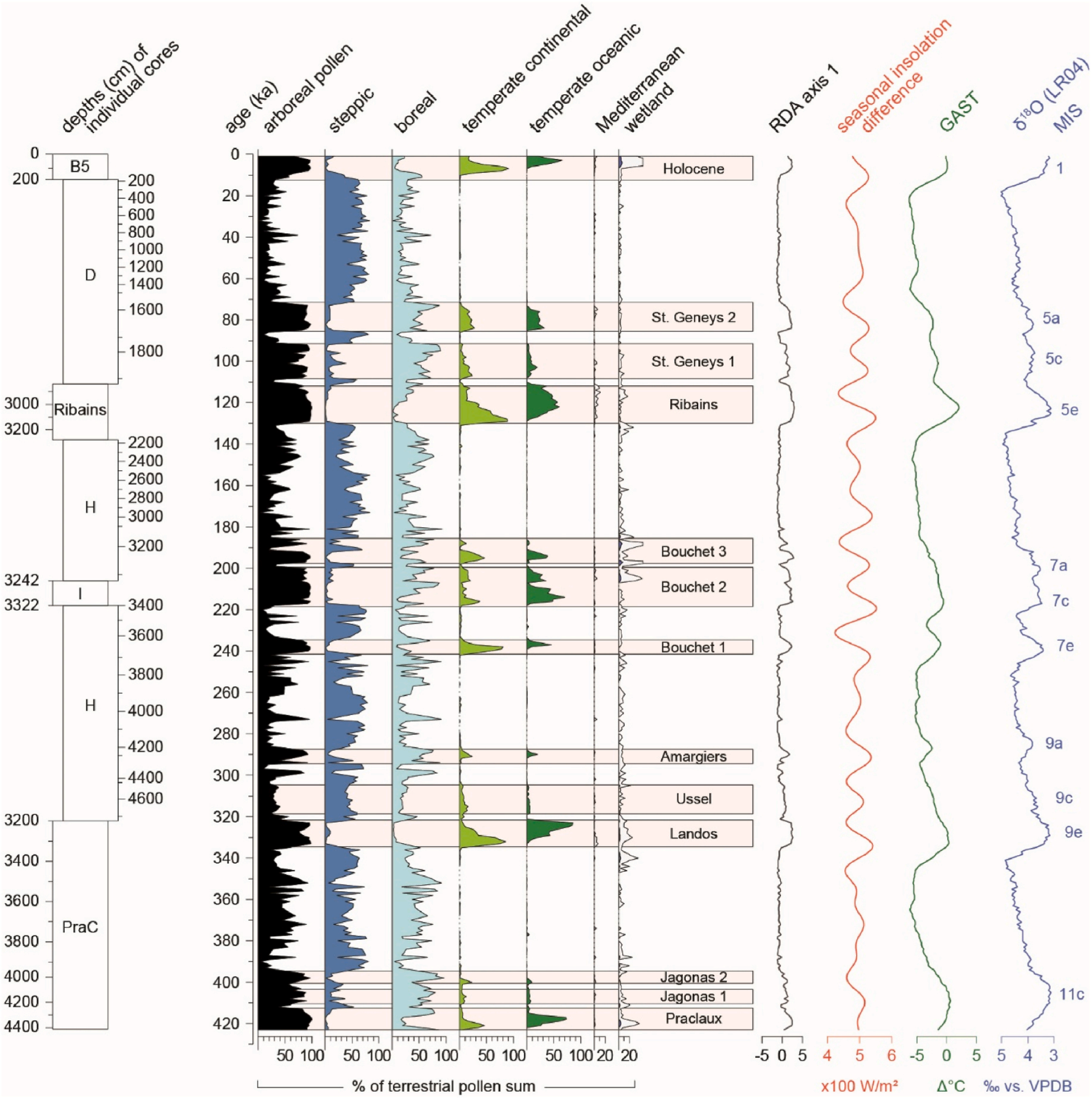

Fig. 4. Pooled and interpolated (1 ka resolution) percentages of vegetation types based on pollen percentages (see Table 2) of the Velay composite profile. Depth ranges (on age scale) of all cores used for the composite profile (see Table 1) are shown on the left. Climate proxies are: $\delta^{18}O$ (LR04) = global benthic oxygen isotope record (Lisiecki and Raymo, 2005); GAST = Global average surface temperature (Snyder, 2016). Seasonal insolation difference (June–December solstice) was calculated for 65°N using the la04 solution (Laskar et al., 2004). $\delta^{18}O$ values are shown as ‰ vs. the standard Vienna Pee Dee Belemnite (VPDB) on reversed scales. GAST reconstructions are shown as temperature deviation from present (Δ°C). All marine isotope stages (MIS) relevant for the text are labelled according to Lisiecki and Raymo (2005).

Allen et al., 1999; Tzedakis et al., 2001) and therefore deglacial-to-glacial transitions could not be used when tuning terrestrial to marine records. Tuning the Velay record to a terrestrial chronology allowed us to bypass this problem. Interestingly, the new age-depth model generally matches the one previously published (Fig. 3). Most striking is the good correspondence of both age-depth models at the onset of the mesocratic phase (first peak in AP-*Pinus*) of Ribains (MIS 5e) and Praclaux (MIS 11c) (for definition of interglacial stages such as mesocratic or oligocratic see Lang et al., 2023). However, according to our new model, the mesocratic (early-temperate) phases of the interglacials Landos (MIS 9e) and Bouchet 1 (MIS 7e) started c. 4 ka, and those of the Holocene (MIS 1) and the Bouchet 3 interstadial (MIS 7a) c. 2 ka later than originally suggested. Due to an inferred hiatus at around 220 ka, the onset of the mesocratic phase of the Bouchet 2 interstadial (MIS 7c) is not recorded in the original model. Using our new composite profile, however, allows to capture this phase, which likely occurred at least 1–2 ka later than previously suggested. The mesocratic phase of interstadials Amargiers (MIS 9a) and St. Geneys 1 (MIS 5c) occurred earlier (c. 4 ka) according to our new model. The duration of the forested phases during the interstadials Bouchet 3 (MIS 7a), St. Geneys 1 (MIS 5c), and St. Geneys 2 (MIS 5a) appear longer according to our calibration, but apparently the duration of Praclaux (MIS 11c) is shorter. Indeed, the Praclaux interglacial ends with a hiatus of unknown length in the older model, whereas we suggest that it ends at least 8 ka earlier. The hiatus was also affecting the subsequent Jagonas interstadial (MIS 11a) in the original age assignment. Hence, no temporal comparison is possible for this part of the section.

3.2. Successional patterns of vegetation types in the Massif Central

The general successional patterns of the vegetation types at Velay can be attributed to the glacial-interglacial cycles, i.e., the cryocratic (glacial), protocratic (pre-temperate), mesocratic (early-temperate), oligocratic (late-temperate), and the telocratic (post-temperate) phases (Iversen, 1958; Andersen, 1964; Birks and Birks, 2004; Birks and Tinner, 2016) (Fig. 4). The cryocratic phases are characterized by predominant steppic (mainly Poaceae, *Artemisia*, and Chenopodiaceae) and boreal (i.e., *Pinus*) vegetation. At the onset of interglacials and interstadials, a short phase with domination of boreal vegetation marks the protocratic phase. Subsequently, temperate continental taxa are the most abundant taxa during the mesocratic phases. *Corylus* is a major constituent of this phase only during interglacials, whereas during interstadials, deciduous *Quercus* is the dominant temperate taxon (Fig. S1). The only exceptions are the Bouchet 2 and 3 interstadials, during which *Corylus* remains at similar levels as *Quercus*. This difference is possibly related to legacy effects. In contrast to Bouchet 1, the interstadials Bouchet 2 and Bouchet 3 were preceded by stadials, which were warm and/or short enough for *Quercus* to remain in the region, thereby possibly giving it a migrational advantage over *Corylus* during subsequent interstadials. Alternatively, only during early interglacials summers were hot and dry enough to allow *Corylus* to dominate the vegetation (Tinner and Lotter, 2001; Finsinger et al., 2006). Subsequently, during oligocratic interglacial phases, temperate oceanic taxa such as *Fagus* and/or *Abies* dominated the forest composition. Except for the Praclaux Interglacial, less oceanic *Carpinus* usually expanded earlier than *Abies* and *Fagus*, i.e., at the transition between the mesocratic and oligocratic phases.

3.3. Redundancy Analysis (RDA)

RDA axis 1, the main gradient reflecting compositional change, explains more of the total variance at Velay (32.74 %) than at Lake Ohrid (24.94 %) (Fig. 5a and b). RDA axis 2 explains 1.68 % at Velay and 2.72 % at Lake Ohrid. In both cases, the explained variance by axis 1 and 2 is significant at a 0.01 confidence level (Table 4). Temperature explains the gradient along axis 1 for both sites, as evidenced by the close alignment of both temperature proxies along this axis. At both sites, the largest values along axis 1 are reached by the MIS 5e equivalents Ribains (Velay) and OD-3e (Lake Ohrid), although more distinctly at Velay. MIS 11c, MIS 9e, and MIS 1 equivalents have intermediate axis 1 values. The MIS 7e equivalents Bouchet 1 (Velay) and OD-6e (Lake Ohrid) show the lowest sample scores along axis 1. All interglacials of Velay are evenly distributed along axis 2, while at Lake Ohrid interglacials OD-3e (MIS 5e) and OD-10c (MIS 11c) are separated from the remaining

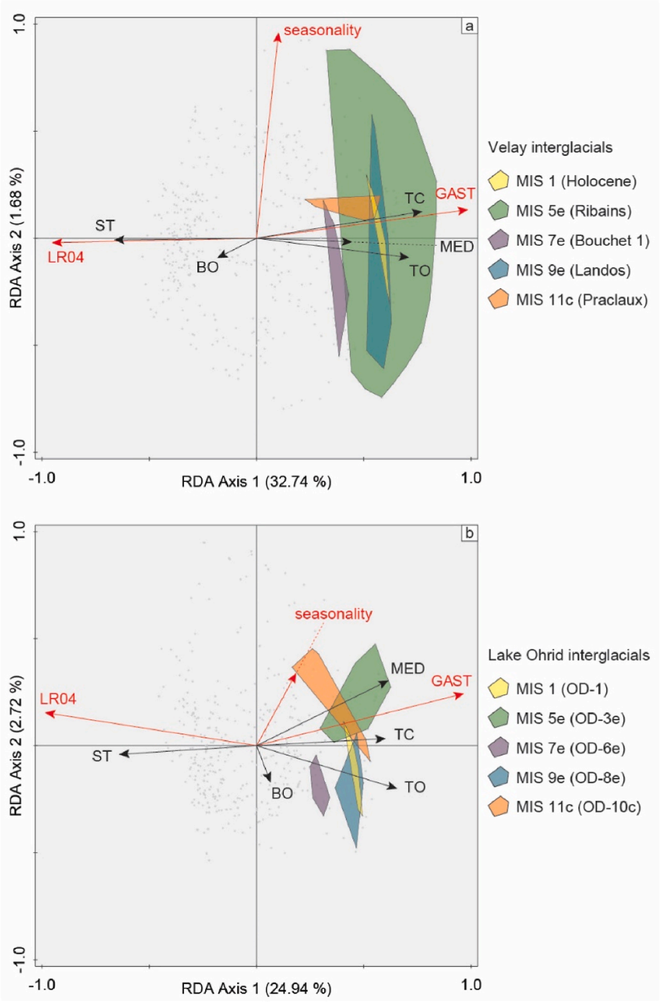

Fig. 5. Redundancy Analysis (RDA) with pooled and interpolated samples (grey dots) of **a.** Velay and **b.** Lake Ohrid (Donders et al., 2021). Envelopes include samples from interglacial optimum phases (see methods). Scores of vegetation types Mediterranean (MED), temperate continental (TC), temperate oceanic (TO), boreal (BO) and steppic (ST) are shown as black arrows. Explanatory variables are represented by red arrows and read LR04 = global benthic δ^{18}O stack (Lisiecki and Raymo, 2005), GAST = global average surface temperature stack (Snyder, 2016), and seasonality = insolation difference between summer and winter solstice. Note that opposite directions along axis 1 realized by benthic δ^{18}O values and GAST reconstructions are related to their inverse relation with temperature (more positive δ^{18}O values indicate cooler conditions).

Table 4
Explained variance by and significance of RDA axes and explanatory variables.

% of total variance explained by	Velay	Lake Ohrid
RDA axis 1	32.74	24.94
RDA axis 2	1.68	2.72
LR04	29.8	24.3
GAST	31.8	23.5
Seasonal insolation difference	1.9	1.9

interglacials on the positive segment of axis 2. This pattern can be interpreted as driven by differences in the seasonal insolation, which is positively aligned with axis 2 (Fig. 5b). Interestingly, of the two interglacials MIS 11c and 5e, only MIS 5e had a strong positive anomaly of summer insolation (precession minimum), resulting in high seasonality values. In fact, summer insolation forcing at the onset of MIS 11c was exceptionally low for a deglaciation to occur (known as 'Stage 11 problem'; Imbrie et al., 1984; Tzedakis et al., 2022). Hence, a more probable explanation for the separation of MIS 5e and MIS 11c from other interglacials are the exceptionally high temperatures during both interglacials (note that both temperature proxies have positive axis 2 values as well). This is also expressed in the comparably high abundances of Mediterranean taxa during MIS 11c and MIS 5e at Lake Ohrid.

The global benthic δ^{18}O stack (LR04; Velay: 29.8 %; Lake Ohrid: 24.3 %) and the global average surface temperature (GAST; Velay: 31.8 %; Lake Ohrid: 23.5 %) explain most of the variance (Table 4). Seasonal insolation difference accounts for 1.9 % of the variance at both sites. All explanatory variables are significant at a 0.01 confidence level. Both temperature proxies explain more variance at Velay than at Lake Ohrid. We consider that temperature was a more important factor for the growth of temperate deciduous vegetation at the more northern and cooler site of Velay than at the warmer Lake Ohrid site. Indeed, the difference of today's January mean temperature is about 2–3 °C between both sites (c. −5 to 0.5 °C vs. 2.4 °C). Hence, the mean January temperatures at Velay are closer to the lower temperature limit of temperate climatic conditions (−3 °C temperature mean of the coldest month; Kottek et al., 2006). In support of this assignment, warm-temperate or subtropical Mediterranean taxa are less important at Velay (Fig. 5a and Fig. S1) than at Lake Ohrid (Fig. 5b and Fig. S2), which again reflects the different temperature settings. Interestingly, temperate oceanic taxa are dominated by *Carpinus* at the cooler Velay site, and by *Abies* at Lake Ohrid, where climate is warmer.

3.4. Response curves

Vegetation changes on glacial-interglacial timescales are closely coupled with orbitally driven temperature oscillations (c. 100 ka cycles in the Middle and Late Pleistocene). Hence, vegetation assemblages are usually stable during glacial periods with durations of roughly 80 to 90 ka. During the same time, and due to the higher frequencies of the obliquity (c. 41 ka) and precession (c. 21 ka) cycles, seasonality experiences several local maxima and minima. This decoupling of seasonality and vegetation changes over full glacial-interglacial cycles is mirrored in our RDA results, which do not delimit seasonality as a major driver of vegetation changes over the last 423 ka. In contrast, if only interglacial periods are considered, all vegetation groups except for wetland taxa at Lake Ohrid respond significantly to seasonality (seasonal insolation difference) at both sites (Fig. 6; left panel). Generally, temperate continental taxa (e.g., deciduous *Quercus*, *Corylus*) increase and temperate oceanic taxa (e.g., *Abies, Carpinus*) decrease with higher seasonality (i.e., lower abundances towards more positive values on the x-axes). Mediterranean taxa (e.g., *Quercus ilex*, *Q. cerris*, *Ostrya/Carpinus orientalis*) show a slight negative trend towards high seasonality at Velay and highest abundances with increased seasonality at Lake Ohrid. Responses of temperate continental and temperate oceanic taxa are generally more pronounced at Velay compared with Lake Ohrid, which might be related

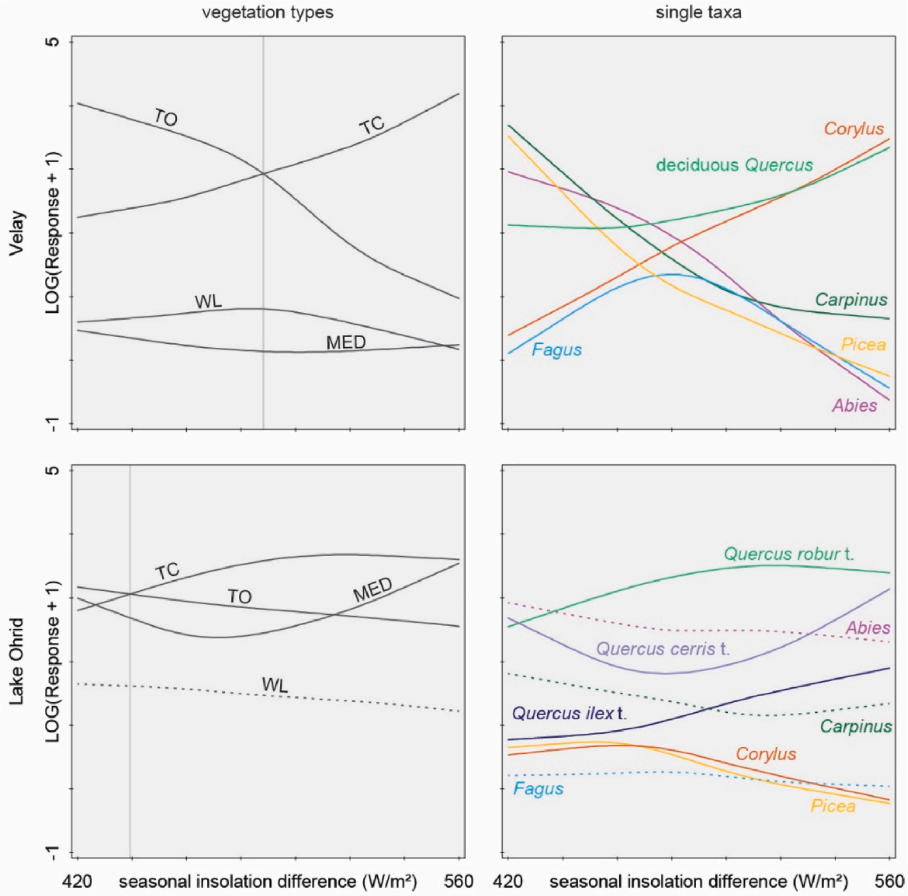

Fig. 6. Response curves of vegetation types (TC: temperate continental, TO: temperate oceanic, MED: Mediterranean, WL: wetland) (left panel) and selected pollen taxa (right panel) to seasonal insolation difference for Velay (top) and Lake Ohrid (bottom). All response curves were fitted using a Generalized Additive Model (GAM) considering only interglacial samples of both records (see methods). Dashed response curves are used if the model is not significant at a 5 % confidence level. Vertical grey lines delimit the seasonality threshold for the transition between the predominance of temperate continental and temperate oceanic vegetation.

to the temperature buffering effect of the Mediterranean Sea and/or the large Lake itself (Donders et al., 2021).

In all considered interglacials except MIS 11c, seasonality is highest at the beginning and steadily decreases afterwards. At the transition from the meso- to the oligocratic phase, seasonality has decreased enough for oceanic taxa to spread. At Lake Ohrid, this threshold is lower than at Velay, where continental taxa (mainly deciduous *Quercus* and *Corylus*) get replaced by oceanic taxa (mainly *Abies* and *Carpinus*) while seasonality is still comparably high (Fig. 6). At Lake Ohrid, however, continental taxa (mainly *Quercus robur* type) have remained even when seasonality gets relatively low, which is most likely an effect related to reduced moisture availability in the sub-Mediterranean climate during summer.

At Velay, all major constituents of the temperate forest biome respond significantly to seasonality (Fig. 6; top right) over five interglacials. This result suggests that species-specific niche preferences remained stable since 423 ka. Temperate continental taxa such as deciduous *Quercus* and *Corylus* strongly profit from increased seasonality, whereas the temperate oceanic taxa *Fagus*, *Carpinus*, and *Abies* as well as boreal *Picea* respond negatively to increased seasonality. The latter of which might be mainly due to reduced moisture availability during summer, to which it is highly susceptible. Unexpectedly, oceanic *Fagus* shows a negative response to low seasonality. Due to their similar niche preferences, this might be explained by the competition with *Abies* for light. At Lake Ohrid, all considered single taxa except temperate oceanic *Abies*, *Carpinus*, and *Fagus* respond significantly to seasonality (Fig. 6; bottom right). In this case, and as mentioned above, the potential of the Mediterranean Sea, and possibly of the large Lake itself, to buffer seasonal temperature differences serves as the most likely explanation.

4. Discussion

4.1. Improvements of the new age-depth model

The differences between our model and the one established by Tzedakis et al. (1997) result from the different underlying tuning targets. Our age-depth model is tuned on the Lake Ohrid sequence, which is constrained by a combination of numerically dated tephra layers and orbital tuning of biogeochemical proxies (Wagner et al., 2017). These constraints result in a numerical and pollen-independent terrestrial chronology. The former age-depth model was tuned on the marine SPECMAP curve (Imbrie et al., 1984). Accordingly, it is likely affected by leads and lags between the marine and the terrestrial realms. However, the extent of asynchrony is still a matter of debate (Sanchez Goñi et al., 1999; Tzedakis et al., 2001, 2004; Shackleton et al., 2003; Desprat et al., 2007, 2009; Naughton et al., 2016).

Sources of potential uncertainties in our approach are lags between the vegetational responses to climate change in the Massif Central compared to the Balkan Peninsula. Site-specific delays of the forest expansion at the onset of interglacials might lead to an underestimation of the new Velay ages (i.e., if the forest in fact expanded later in the Massif Central compared with the Balkan Peninsula). However, both sites are closely situated to glacial refugial areas (Lang et al., 2023). Therefore, migrational lags can be considered minimal (Tzedakis et al., 1997) and within the uncertainties of the Lake Ohrid chronology. This interpretation is supported by the independently dated afforestation during the Early Holocene at both sites (Fig. 2). An additional source of uncertainty is the fact that our tuning approach bases on linear interpolations between tie points, hence assuming constant sedimentation rates. The assumption is an idealized view on sedimentary processes (Blaauw, 2012), especially if the tie points are exclusively set at the beginning of warm phases and the linear interpolation is extended over an entire glacial-interglacial cycle. Hence, the increased number of tie points we used to delimit the end of forested periods constitutes an improvement compared with the previous approach. This especially accounts for the estimation of the duration of forested phases.

Our age depth-model can be tested against independent chronological constraints. One possibility is the Ar/Ar age (275 ± 5 ka), which has been obtained via a tephra layer deposited at Lac du Bouchet during the Amargiers interstadial (Roger et al., 1999). Moreover, a tephra layer from the site of Orgnac 3 (Ardèche, France), which was linked to the same eruption, was dated to 298 ± 55 ka with the fission-track method (Khatib, 1994). Based on our new age-depth model, the bottom of the tephra layer in the Velay composite profile (4300 cm depth in core H; Fig. 4 and Table 1) corresponds to an age of 295 ka, which is in best agreement with the age of the tephra layer from Orgnac 3, but it is in disagreement with the Ar/Ar age from Lac du Bouchet. Biostratigraphic evidence shows that the tephra from Lac du Bouchet was deposited during a period with boreo-nemoral forest vegetation (*Pinus*, *Betula*, *Quercus*, *Corylus*, and *Carpinus*; Lang et al., 2023). The tephra layer itself contains a large amount of pollen grains, mainly *Carpinus* (70 %; Reille and Beaulieu, 1995). Interestingly, climate proxy data ($\delta^{18}O$ and SST; Fig. 4) suggest that the Ar/Ar age of 275 ± 5 ka corresponds to a cold period during MIS 8. During such conditions, it is very unlikely that temperate deciduous trees and shrubs would have established at Velay. Hence, the Ar/Ar age of the tephra at Velay appears c. 20 ka too young.

4.2. Interglacial vegetation responses since 423 ka

A combination of orbital configuration and greenhouse gas concentrations resulted in comparably warm (MIS 5e, MIS 11c), intermediate (MIS 1, MIS 9e), and rather cool (MIS 7e) interglacials (Tzedakis et al., 2009; Past Interglacials Working Group of PAGES, 2016). These differences between interglacial climates are expressed at both sites, although the processes varied locally due to the different climatic regimes. The particularly warm interglacial MIS 5e shows vegetation assemblages that are statistically distinguishable from other interglacials (Fig. 5a and b). Warm climate promoted the increased presence of Mediterranean taxa at Lake Ohrid (Fig. S2), which likely occupied higher-than-today elevations in the catchment at that time (Lézine et al., 2010; Sadori et al., 2016). At Velay, however, a shift towards higher temperatures might have favoured Mediterranean taxa to spread north along the Rhone Valley closer to the study site, but most likely they were never growing locally at the site itself (Beaulieu and Reille, 1992) (Fig. S1). Instead, we infer that the warm MIS 5e interglacial climate resulted in higher abundances of rather oceanic (*Carpinus* and *Taxus*) and rather continental (e.g., deciduous *Quercus* and *Corylus*) temperate taxa (Fig. S1). In addition, the warm and possibly seasonally dry climate may have caused low abundances of wetland taxa at Velay (Fig. S1). Based on these results, we suggest that for Mediterranean taxa to spread into the temperate forest biome of Central Europe, future climate warming will have to exceed at least the MIS 5e global surface temperature anomaly of +1.3 °C (compared with pre-industrial Holocene levels; Fischer et al., 2018).

MIS 11c was similarly warm as MIS 5e (Past Interglacials Working Group of PAGES, 2016). Nevertheless, the vegetation assemblage of MIS 11c was more similar to MIS 1 and MIS 9e than to MIS 5e at both sites (intermediate RDA axis 1 values; Fig. 5a and b). Similarly, Cheddadi et al. (2005) suggested a low correspondence between MIS 11c and MIS 5e based on bioclimatic affinity groups (after Laurent et al., 2004) of the Velay pollen data. Other than MIS 5e, which was particularly warm because of the combined effects of boreal summer insolation and greenhouse gas forcing, the relatively high MIS 11c temperatures were not a result of the comparably low boreal summer insolation forcing (Yin and Berger, 2012, 2015), but can be mainly explained by a response to greenhouse gas concentrations. These were at similarly high levels than during MIS 5e (Loulergue et al., 2008; Lüthi et al., 2008). As a result, Mediterranean *Quercus ilex* and temperate continental taxa such as *Corylus*, deciduous *Quercus*, *Ulmus*, *Fraxinus*, *Acer*, and *Tilia*, were less abundant during MIS 11c (low seasonality) than during MIS 5e (high seasonality) in Velay. Instead, *Abies* could thrive under these more oceanic conditions of MIS 11c and, by an early occupation of the habitats, possibly prevented the establishment of *Carpinus*. Farther south at Lake Ohrid, the combination of particularly warm temperatures and high seasonality during MIS 5e resulted in higher abundances of Mediterranean taxa such as *Quercus cerris* and *Ostrya/Carpinus orientalis* compared to MIS 11c. These findings imply that summer temperatures were important and that precession-driven seasonality of moisture availability may have influenced forest expansions in the Mediterranean (Oliveira et al., 2018). Unexpectedly, continental deciduous oaks (*Q. robur* type) were less abundant during MIS 5e (high seasonality) compared with MIS 11c (low seasonality), while the opposite is the case for more oceanic *Carpinus*. This finding implies that other factors than seasonality played a crucial role in determining the forest composition in the sub-Mediterranean biome, as also highlighted by the results of the response curves (Fig. 6). Indeed, Oliveira et al. (2018) found different vegetation compositions during the astronomically very similar MIS 11c and MIS 1 in a marine sequence of SW Iberia, which the authors explain by an amplified latitudinal insolation and a resulting thermal disparity between MIS 11c and MIS 1.

Low obliquity during MIS 7e is considered to have caused low summer insolation (Past Interglacials Working Group of PAGES, 2016), which resulted in rather low summer temperatures compared with other interglacials (see also δ^{18}O and GAST in Fig. 4). During this period, the vegetation composition at both sites was statistically different from that of other interglacials, as shown by the lowest values along RDA axis 1 (Fig. 5). At Lake Ohrid, conditions were less favourable for Mediterranean plants to colonize higher altitudes. Instead, temperate oceanic taxa prevailed, and *Abies* was even more pronounced during MIS 7e than MIS 5e, when it reached high values together with Mediterranean taxa such as *Quercus ilex* type and *Q. cerris* type (Fig. S2). At Velay, a less pronounced oligocratic (late-temperate) phase with negligible presence of *Abies* and *Taxus* characterizes MIS 7e, while the mesocratic (early-temperate) phase was less affected. This assumption of reduced effects on the vegetation of the mesocratic stage is based on the abundances of temperate continental taxa such as *Quercus* and *Corylus*, which reach similar levels as during warm interglacials (Fig. S1). In fact, of the temperate oceanic vegetation type, only *Carpinus* was similarly dominant as during other interglacials, reflecting its requirements for slightly more continental conditions compared with *Abies* (Landolt et al., 2010). The either too short or too cold climate optimum phase of MIS 7e at Velay prevented a late-temperate vegetation to develop. Yet, and similar to the trend in Southern Europe, MIS 7e clearly has an interglacial character in the Velay record, and the discussion whether it was an interstadial or an interglacial may mainly concern higher latitudes (Tzedakis et al., 2004).

Based on the Velay data, Cheddadi et al. (2005) found that the vegetation during MIS 5e and MIS 7e were relatively similar. This stands in contrast to our findings and to the fundamentally different climatic signatures of these warm phases. This difference in views most likely reflects the response of the different approaches that were used to measure similarity. In particular, while our analysis bases on the ecology of dominant or co-dominant single taxa, Cheddadi et al. (2005) based their interpretation on bioclimatic affinity groups, which integrate pollen types according to the morphology, phenology, and climatic requirements of the assumed plant species.

Sanchez Goñi et al. (2018) suggested that the expansion of Mediterranean forest assemblages south of 40°N are mostly driven by precessional-driven winter precipitation, whereas temperate forests farther north are mainly influenced by obliquity-driven annual temperatures. In agreement, the important role of moisture availability on Mediterranean biome shifts has been demonstrated at Tenaghi Philippon (40 m a.s.l.), a site at the transition between meso-Mediterranean and sub-Mediterranean vegetation types in Greece (Koutsodendris et al., 2023). Lake Ohrid is located only slightly north of 40°N and indeed temperatures generally explain less variance of the compositional changes (RDA axis 1) compared with Velay (Table 4). However, Lake Ohrid is a temperate sub-Mediterranean site with continental influence, where harsh winter conditions and (late) frost primarily determine the occurrence (or today total lack) of Mediterranean evergreen broadleaved trees such as *Quercus ilex*, *Pistacia lentiscus*, and *Olea europaea*. In agreement, our RDA-analysis shows a high relevance of temperature changes for vegetation composition at Lake Ohrid and GAM response curves to seasonality reveal that the difference between the warm and the cold season was species-specific, likely co-promoting vegetation shifts. The impact of temperature vs. moisture changes on forestation (% AP) at Lake Ohrid has been discussed in Donders et al. (2021). On the basis of a comparison with modelled temperature and moisture data, the authors came to the conclusion that temperature changes accounted for more variation on longer (i.e., glacial-interglacial) timescales, while moisture availability was more important on shorter precessional timescales. Nevertheless, while the importance of temperature is clear, assessing the direct effect of moisture availability at Lake Ohrid is currently more complicated. Going beyond a comparison of pollen data with simulated climate data would require local and pollen-independent time series on palaeo-moisture.

5. Conclusions

We have established a new age depth-model for the long sequence at Velay, the most complete European terrestrial pollen record of the last 423 ka outside the Mediterranean region. Compared with the previous model, we used a larger number of tie points, which results in higher chronological accuracy. Additionally, improvements could be achieved by considering numerical ages established on tephra layers and using a terrestrial record as tuning target, which is geographically closer to the Massif Central than tuning those targets that have previously been used. For the first time, ordination techniques with climate proxy data as explanatory variables numerically document the importance of temperatures in driving vegetation changes in the Massif Central and the Balkan Peninsula over several glacial-interglacial cycles. In fact, our results suggest that temperature was the main driver of vegetation composition at both sites, although moisture possibly played a more important role at the more southern Lake Ohrid site. Interglacial vegetation responses to Middle and Late Pleistocene climate change followed similar patterns in the Massif Central and in the Balkan region. Particularly warm or cool interglacials resulted in distinct vegetation assemblages. In the Massif Central, temperate oceanic taxa such as *Abies*, *Taxus*, and to a lesser extent *Carpinus*, were most affected by variations of interglacial intensity, while in the Balkans, the same accounts for more thermophilous meso- and submediterranean taxa such as *Quercus ilex*, *Quercus cerris*, or *Ostrya/Carpinus orientalis*. Responses to seasonality of single taxa as well as vegetation groups were roughly consistent over five interglacials and suggest that species-specific niche preferences have remained constant since at least 423 ka. We additionally use the vegetation composition during the Eemian (MIS 5e) at Velay and at Lake Ohrid to propose that evergreen broadleaved Mediterranean taxa (e.g., *Quercus ilex*) will not expand north of the Alps unless future climates exceed the MIS 5e warming of c. +1.3 °C if compared to preindustrial Holocene (Fischer et al., 2018). Similarly, we infer that evergreen broadleaved Mediterranean vegetation will not establish at the sub-Mediterranean site Lake Ohrid if climate will remain within the variability of the past 423 ka. Yet, interglacial comparisons suggest that climate change, especially temperature, already at lower magnitudes will cause restructuring of the current vegetation in both biomes in the future.

Author contributions

PS, WT, EG, and HV conceptualized the study. JLdB and MR contributed data. PS performed all analyses, created the artwork, and wrote the first draft of the manuscript. EG, HV, and JLdB commented on the manuscript, WT and FS helped finalizing it. FS acquired the funding.

Declaration of competing interest

The authors declare that they have no known competing financial interests or personal relationships that could have appeared to influence the work reported in this paper.

Data availability

Data will be made available on request.

Acknowledgements

The work of the data contributors and the European Pollen Database (EPD; http://www.europeanpollendatabase.net/) community is gratefully acknowledged. We thank the reviewers for helping to improve the manuscript. The corresponding author was funded by the Swiss National Science Foundation, Switzerland (project number 175555) awarded to Fritz Schlunegger.

Appendix A. Supplementary data

Supplementary data to this article can be found online at https://doi.org/10.1016/j.quascirev.2024.108715.

References

Allen, J.R.M., Brandt, U., Brauer, A., Hubberten, H.-W., Huntley, B., Keller, J., Kraml, M., Mackensen, A., Mingram, J., Negendank, J.F.W., Nowaczyk, N.R., Oberhänsli, H., Watts, W.A., Wulf, S., Zolitschka, B., 1999. Rapid environmental changes in southern Europe during the last glacial period. Nature 400 (6746), 740–743. https://doi.org/10.1038/23432.

Andersen, S.T., 1964. Interglacial Plant Successions in the Light of Environmental Changes: Report of the VIth International Congress on Quaternary, Warsaw 1961, vol. II. Palaeobotanical Section, Łódź.

Beaulieu, J.-L. de, Andrieu-Ponel, V., Reille, M., Grüger, E., Tzedakis, P.C., Svobodova, H., 2001. An attempt at correlation between the Velay pollen sequence and the Middle Pleistocene stratigraphy from central Europe. Quat. Sci. Rev. 20 (16–17), 1593–1602. https://doi.org/10.1016/S0277-3791(01)00027-0.

Beaulieu, J.-L. de, Pons, A., Reille, M., 1984. Recherches pollenanalytiques sur l'histoire de la végétation des Monts du Velay, Massif Central, France. Diss. Bot. 72, 45–70.

Beaulieu, J.-L. de, Reille, M., 1992. Long Pleistocene pollen sequences from the velay plateau (Massif central, France). Veg. Hist. Archaeobotany 1 (4), 233–242. https://doi.org/10.1007/BF00189500.

Bereiter, B., Eggleston, S., Schmitt, J., Nehrbass-Ahles, C., Stocker, T.F., Fischer, H., Kipfstuhl, S., Chappellaz, J., 2015. Revision of the EPICA Dome C CO 2 record from 800 to 600 kyr before present. Geophys. Res. Lett. 42 (2), 542–549. https://doi.org/10.1002/2014GL061957.

Birks, H.J.B., 2019. Contributions of Quaternary botany to modern ecology and biogeography. Plant Ecol. Divers. 12 (3–4), 189–385.

Birks, H.J.B., Birks, H.H., 2004. The rise and fall of forests. Science 305 (5683), 484–485. https://doi.org/10.1126/science.1101357.

Birks, H.J.B., Tinner, W., 2016. Past forests of Europe. In: San-Miguel-Ayanz, J., Rigo, D. de, Caudullo, G., Durrant, T.H., Mauri, A. (Eds.), European Atlas of Forest Tree Species. Publication Office of the European Union, Luxembourg, pp. 36–39.

Bittmann, F., 1992. The Kärlich interglacial, Middle Rhine region, Germany: vegetation history and stratigraphic position. Veg. Hist. Archaeobotany 1, 243–258. https://doi.org/10.1007/bf00189501.

Blaauw, M., 2012. Out of tune: the dangers of aligning proxy archives. Quat. Sci. Rev. 36, 38–49. https://doi.org/10.1016/j.quascirev.2010.11.012.

Böhling, N., Greuter, W., Raus, T., 2002. Indicator values for vascular plants in the Southern Aegean (Greece). Braun-Blanquetia 32, 1–106. https://scholar.google.com/citations?user=h7ajsgcaaaaj&hl=de&oi=sra.

Brechbühl, S., van Vugt, L., Gobet, E., Morales-Molino, C., Volery, J., Lotter, A.F., Ballmer, A., Brugger, S.O., Szidat, S., Hafner, A., Tinner, W., 2023. Vegetation dynamics and land-use change at the neolithic lakeshore settlement site of Ploča Mičov Grad, Lake Ohrid, north Macedonia. Veg. Hist. Archaeobotany 1–21. https://doi.org/10.1007/s00334-023-00931-3.

Cheddadi, R., Beaulieu, J.-L. de, Jouzel, J., Andrieu-Ponel, V., Laurent, J.-M., Reille, M., Raynaud, D., Bar-Hen, A., 2005. Similarity of vegetation dynamics during interglacial periods. P Natl Acad Sci USA 102 (39), 13939–13943. https://doi.org/10.1073/pnas.0501752102.

Crucifix, M., 2016. Palinsol: Insolation for Palaeoclimate Studies.

Desprat, S., Sanchez Goñi, M.F., McManus, J.F., Duprat, J., Cortijo, E., 2009. Millennial-scale climatic variability between 340 000 and 270 000 years ago in SW Europe: evidence from a NW Iberian margin pollen sequence. Clim. Past 5 (1), 53–72. https://doi.org/10.5194/cp-5-53-2009.

Desprat, S., Sanchez Goñi, M.F., Naughton, F., Turon, J.-L., Duprat, J., Malaizé, B., Cortijo, E., Peypouquet, J.-P., 2007. 25. Climate variability of the last five isotopic interglacials: direct land-sea-ice correlation from the multiproxy analysis of North-Western Iberian margin deep-sea cores. In: Sirocko, F., Claussen, M., Sanchez Goñi, M.F., Litt, T. (Eds.), Developments in Quaternary Sciences: the Climate of Past Interglacials. Elsevier, pp. 375–386.

Desprat, S., Sanchez Goñi, M.F., Turon, J.-L., Duprat, J., Malaizé, B., Peypouquet, J.-P., 2006. Climatic variability of Marine Isotope Stage 7: direct land–sea–ice correlation from a multiproxy analysis of a north-western Iberian margin deep-sea core. Quat. Sci. Rev. 25 (9–10), 1010–1026. https://doi.org/10.1016/j.quascirev.2006.01.001.

Desprat, S., Sanchez Goñi, M.F., Turon, J.-L., McManus, J.F., Loutre, M.-F., Duprat, J., Malaizé, B., Peyron, O., Peypouquet, J.-P., 2005. Is vegetation responsible for glacial inception during periods of muted insolation changes? Quat. Sci. Rev. 24 (12–13), 1361–1374. https://doi.org/10.1016/j.quascirev.2005.01.005.

Donders, T.H., Panagiotopoulos, K., Koutsodendris, A., Bertini, A., Mercuri, A.M., Masi, A., Combourieu-Nebout, N., Joannin, S., Kouli, K., Kousis, I., Peyron, O., Torri, P., Florenzano, A., Francke, A., Wagner, B., Sadori, L., 2021. 1.36 million years of Mediterranean forest refugium dynamics in response to glacial-interglacial cycle strength. P Natl Acad Sci USA 118 (34), e2026111118. https://doi.org/10.1073/pnas.2026111118.

Ellenberg, H., 2009. Vegetation Ecology of Central Europe. Cambridge Univ. Press, Cambridge.

European Environment Agency, 2016. Biogeographical regions in Europe. https://www.eea.europa.eu/data-and-maps/figures/biogeographical-regions-in-europe-2.

Finsinger, W., Tinner, W., van der Knaap, W.O., Ammann, B., 2006. The expansion of hazel (Corylus avellana L.) in the southern Alps: a key for understanding its early Holocene history in Europe? Quat. Sci. Rev. 25 (5–6), 612–631. https://doi.org/10.1016/j.quascirev.2005.05.006.

Fischer, H., Meissner, K.J., Mix, A.C., Abram, N.J., Austermann, J., Brovkin, V., Capron, E., Colombaroli, D., Daniau, A.-L., Dyez, K.A., 2018. Palaeoclimate constraints on the impact of 2 °C anthropogenic warming and beyond. Nat. Geosci. 11 (7), 474. https://doi.org/10.1038/s41561-018-0146-0.

Follieri, M., Magri, D., Sadori, L., 1988. 250,000-year pollen record from Valle di Castiglione (Roma). Pollen Spores 30, 329–356.

Francke, A., Wagner, B., Just, J., Leicher, N., Gromig, R., Baumgarten, H., Vogel, H., Lacey, J.H., Sadori, L., Wonik, T., Leng, M.J., Zanchetta, G., Sulpizio, R., Giaccio, B., 2016. Sedimentological processes and environmental variability at Lake Ohrid (Macedonia, Albania) between 637 ka and the present. Biogeosciences 13 (4), 1179–1196. https://doi.org/10.5194/bg-13-1179-2016.

Geyh, M.A., Müller, H., 2005. Numerical 230Th/U dating and a palynological review of the Holsteinian/Hoxnian Interglacial. Quat. Sci. Rev. 24 (16–17), 1861–1872. https://doi.org/10.1016/j.quascirev.2005.01.007.

Hastie, T., Tibshirani, R., 1999. Generalized additive models. In: Monographs on Statistics and Applied Probability 43. Chapman & Hall, London, New York.

Herzschuh, U., Birks, H.J.B., Laepple, T., Andreev, A., Melles, M., Brigham-Grette, J., 2016. Glacial legacies on interglacial vegetation at the Pliocene-Pleistocene transition in NE Asia. Nat. Commun. 7 (1), 1–11. https://doi.org/10.1038/ncomms11967.

Iversen, J., 1958. The bearing of glacial and interglacial epochs on the formation and extinction of plant taxa. Syst Today Uppsala Univ Årsskr 6, 210–215.

Imbrie, J., Berger, A., Boyle, E.A., Clemens, S.C., Duffy, A., Howard, W.R., Kukla, G., Kutzbach, J., Martinson, D.G., McIntyre, A., Mix, A.C., Molfino, B., Morley, J.J., Peterson, L.C., Pisias, N.G., Prell, W.L., Raymo, M.E., Shackleton, N.J., Toggweiler, J.R., 1984. The orbital theory of Pleistocene climate: support from a revised chronology of the marine d18O record.

Khatib, S., 1994. Datations des cendres volcaniques et analyses géochimiques du remplissage d'Orgnac 3 (Ardèche, France). quate 5 (1), 13–22. https://doi.org/10.3406/quate.1994.2010.

Kottek, M., Grieser, J., Beck, C., Rudolf, B., Rubel, F., 2006. World Map of the Köppen-Geiger climate classification updated. metz 15 (3), 259–263. https://doi.org/10.1127/0941-2948/2006/0130.

Koutsodendris, A., Dakos, V., Fletcher, W.J., Knipping, M., Kotthoff, U., Milner, A.M., Müller, U.C., Kaboth-Bahr, S., Kern, O.A., Kolb, L., Vakhrameeva, P., Wulf, S., Christanis, K., Schmiedl, G., Pross, J., 2023. Atmospheric CO2 forcing on Mediterranean biomes during the past 500 kyrs. Nat. Commun. 14 (1), 1664. https://doi.org/10.1038/s41467-023-37388-x.

Lamothe, M., 2016. Luminescence dating of interglacial coastal depositional systems: recent developments and future avenues of research. Quat. Sci. Rev. 146, 1–27. https://doi.org/10.1016/j.quascirev.2016.05.005.

Landolt, E., Bäumler, B., Erhardt, O., Klötzli, F., Lämmler, W., Nobis, M., Rudmann-Maurer, K., Schweingruber, F.H., Theurillat, J.-P., Urmi, E., Vust, Mathias, Wohlgemuth, Thomas, 2010. Flora indicativa: Ökologische Zeigerwerte und biologische Kennzeichen zur Flora der Schweiz und der Alpen, second ed. Haupt, Bern, Stuttgart, Wien.

Lang, G., Ammann, B., Behre, K.-E., Tinner, W. (Eds.), 2023. Quaternary Vegetation Dynamics of Europe, 1, Auflage ed. Haupt, Bern.

Laskar, J., Robutel, P., Joutel, F., Gastineau, M., Correia, A.C.M., Levrard, B., 2004. A long-term numerical solution for the insolation quantities of the Earth. A&A 428 (1), 261–285. https://doi.org/10.1051/0004-6361:20041335.

Laurent, J.-M., Bar-Hen, A., François, L., Ghislain, M., Cheddadi, R., 2004. Refining vegetation simulation models: from plant functional types to bioclimatic affinity groups of plants. J. Veg. Sci. 15 (6), 739–746. https://doi.org/10.1111/j.1654-1103.2004.tb02316.x.

Lézine, A.-M., Grafenstein, U. von, Andersen, N., Belmecheri, S., Bordon, A., Caron, B., Cazet, J.-P., Erlenkeuser, H., Fouache, E., Grenier, C., Huntsman-Mapila, P., Hureau-Mazaudier, D., Manelli, D., Mazaud, A., Robert, C., Sulpizio, R., Tiercelin, J.-J., Zanchetta, G., Zeqollari, Z., 2010. Lake Ohrid, Albania, provides an exceptional multi-proxy record of environmental changes during the last glacial–interglacial cycle. Palaeogeogr. Palaeoclimatol. Palaeoecol. 287 (1–4), 116–127. https://doi.org/10.1016/j.palaeo.2010.01.016.

Lian, O.B., Roberts, R.G., 2006. Dating the Quaternary: progress in luminescence dating of sediments. Quat. Sci. Rev. 25 (19–20), 2449–2468. https://doi.org/10.1016/j.quascirev.2005.11.013.

Lisiecki, L.E., Raymo, M.E., 2005. A Pliocene-Pleistocene stack of 57 globally distributed benthic δ^{18}O records. Paleoceanography 20. https://doi.org/10.1029/2004PA001071.

Loulergue, L., Schilt, A., Spahni, R., Masson-Delmotte, V., Blunier, T., Lemieux, B., Barnola, J.-M., Raynaud, D., Stocker, T.F., Chappellaz, J., 2008. Orbital and millennial-scale features of atmospheric CH4 over the past 800,000 years. Nature 453 (7193), 383–386. https://doi.org/10.1038/nature06950.

Lüthi, D., Le Floch, M., Bereiter, B., Blunier, T., Barnola, J.-M., Siegenthaler, U., Raynaud, D., Jouzel, J., Fischer, H., Kawamura, K., Stocker, T.F., 2008. High-resolution carbon dioxide concentration record 650,000-800,000 years before present. Nature 453 (7193), 379–382. https://doi.org/10.1038/nature06949.

Matevski, V., Čarni, A., Avramoski, O., Juvan, N., Kostadinovski, M., Košir, P., Paušič, A., Šilc, U., 2011. Forest vegetation of Galičica mountain range in Macedonia. ZRC SAZU, Založba ZRC.

Météo France, 2022. Climat Le Puy-Loudes. https://meteofrance.com/climat/releves/france/auvergne-rhone-alpes/le%20puy-loudes.

Naughton, F., Sanchez Goñi, M.F., Rodrigues, T., Salgueiro, E., Costas, S., Desprat, S., Duprat, J., Michel, E., Rossignol, L., Zaragosi, S., Voelker, A., Abrantes, F., 2016. Climate variability across the last deglaciation in NW Iberia and its margin. Quat. Int. 414, 9–22. https://doi.org/10.1016/j.quaint.2015.08.073.

Oliveira, D., Desprat, S., Yin, Q.Z., Naughton, F., Trigo, R., Rodrigues, T., Abrantes, F., Sanchez Goñi, M.F., 2018. Unraveling the forcings controlling the vegetation and climate of the best orbital analogues for the present interglacial in SW Europe. Clim. Dynam. 51 (1–2), 667–686. https://doi.org/10.1007/s00382-017-3948-7.

Parrenin, F., Masson-Delmotte, V., Köhler, P., Raynaud, D., Paillard, D., Schwander, J., Barbante, C., Landais, A., Wegner, A., Jouzel, J., 2013. Synchronous change of atmospheric CO2 and Antarctic temperature during the last deglacial warming. Science 339 (6123), 1060–1063. https://doi.org/10.1126/science.1226368.

Past Interglacials Working Group of PAGES, 2016. Interglacials of the last 800,000 years. Rev. Geophys. 54 (1), 162–219.

Pignatti, S., 2005. Valori di bioindicazione delle piante vascolari della flora d'Italia. Braun-Blanquetia 39, 3–97.

Railsback, L.B., Gibbard, P.L., Head, M.J., Voarintsoa, N.R.G., Toucanne, S., 2015. An optimized scheme of lettered marine isotope substages for the last 1.0 million years, and the climatostratigraphic nature of isotope stages and substages. Quat. Sci. Rev. 111, 94–106. https://doi.org/10.1016/j.quascirev.2015.01.012.

Reille, M., Andrieu, V., Beaulieu, J.-L. de, Guenet, P., Goeury, C., 1998. A long pollen record from Lac du Bouchet, Massif Central, France: For the period ca. 325 to 100 ka BP (OIS 9c to OIS 5e). Quat. Sci. Rev. 17 (12), 1107–1123.

Reille, M., Beaulieu, J.-L. de, 1988. History of the Würm and Holocene vegetation in western velay (Massif Central, France): A comparison of pollen analysis from three corings at Lac du Bouchet. Rev. Palaeobot. Palynol. 54 (3–4), 233–248. https://doi.org/10.1016/0034-6667(88)90016-4.

Reille, M., Beaulieu, J.-L. de, 1990. Pollen analysis of a long upper Pleistocene continental sequence in a Velay maar (Massif Central, France). Palaeogeogr. Palaeoclimatol. Palaeoecol. 80 (1), 35–48.

Reille, M., Beaulieu, J.-L. de, 1995. Long Pleistocene pollen records from the Praclaux crater, south-Central France. Quat. Res. 44 (2), 205–215. https://doi.org/10.1006/qres.1995.1065.

Reille, M., Beaulieu, J.-L. de, Svobodova, H., Andrieu-Ponel, V., Goeury, C., 2000. Pollen analytical biostratigraphy of the last five climatic cycles from a long continental sequence from the Velay region (Massif Central, France). J. Quat. Sci. 15 (7), 665–685.

Roger, S., Féraud, G., Beaulieu, J.-L. de, Thouveny, N., Coulon, C., Jacques Cochemé, J., Andrieu, V., Williams, T., 1999. 40Ar/39Ar dating on tephra of the Velay maars (France): implications for the Late Pleistocene proxy-climatic record. Earth Planet Sci. Lett. 170 (3), 287–299. https://doi.org/10.1016/S0012-821X(99)00115-6.

Roucoux, K.H., Tzedakis, P.C., Frogley, M.R., Lawson, I.T., Preece, R.C., 2008. Vegetation history of the marine isotope stage 7 interglacial complex at Ioannina, NW Greece. Quat. Sci. Rev. 27 (13–14), 1378–1395. https://doi.org/10.1016/j.quascirev.2008.04.002.

Roucoux, K.H., Tzedakis, P.C., Lawson, I.T., Margari, V., 2011. Vegetation history of the penultimate glacial period (Marine isotope stage 6) at Ioannina, north-west Greece. J. Quat. Sci. 26 (6), 616–626. https://doi.org/10.1002/jqs.1483.

Sadori, L., Koutsodendris, A., Panagiotopoulos, K., Masi, A., Bertini, A., Combourieu-Nebout, N., Francke, A., Kouli, K., Joannin, S., Mercuri, A.M., Peyron, O., Torri, P., Wagner, B., Zanchetta, G., Sinopoli, G., Donders, T.H., 2016. Pollen-based paleoenvironmental and paleoclimatic change at Lake Ohrid (south-eastern Europe) during the past 500 ka. Biogeosciences 13 (5), 1423–1437. https://doi.org/10.5194/bg-13-1423-2016.

Sanchez Goñi, M.F., Desprat, S., Fletcher, W.J., Morales-Molino, C., Naughton, F., Oliveira, D., Urrego, D.H., Zorzi, C., 2018. Pollen from the deep-sea: a breakthrough in the mystery of the ice ages. Front. Plant Sci. 9, 38. https://doi.org/10.3389/fpls.2018.00038.

Sanchez Goñi, M.F., Eynaud, F., Turon, J.-L., Shackleton, N.J., 1999. High resolution palynological record off the Iberian margin: direct land-sea correlation for the Last Interglacial complex. Earth Planet Sci. Lett. 171 (1), 123–137. https://doi.org/10.1016/S0012-821X(99)00141-7.

Schläfli, P., Gobet, E., Hogrefe, I., Bittmann, F., Schlunegger, F., Zolitschka, B., Tinner, W., 2023. New vegetation history reconstructions suggest a biostratigraphic assignment of the lowermost Rodderberg interglacial (Germany) to MIS 11. Quat. Sci. Rev. 302, 107932 https://doi.org/10.1016/j.quascirev.2022.107932.

Schläfli, P., Gobet, E., van Leeuwen, J.F., Vescovi, E., Schwenk, M.A., Bandou, D., Douillet, G.A., Schlunegger, F., Tinner, W., 2021. Palynological investigations reveal Eemian interglacial vegetation dynamics at Spiezberg, Bernese Alps, Switzerland. Quat. Sci. Rev. 263, 106975 https://doi.org/10.1016/j.quascirev.2021.106975.

Shackleton, N.J., Sanchez Goñi, M.F., Pailler, D., Lancelot, Y., 2003. Marine Isotope Substage 5e and the Eemian Interglacial. Global Planet. Change 36 (3), 151–155. https://doi.org/10.1016/S0921-8181(02)00181-9.

Shaffer, J.P., 1995. Multiple hypothesis testing. Annu. Rev. Psychol. 46 (1), 561–584. https://doi.org/10.1146/annurev.ps.46.020195.003021.

Sinopoli, G., Masi, A., Regattieri, E., Wagner, B., Francke, A., Peyron, O., Sadori, L., 2018. Palynology of the last interglacial complex at Lake Ohrid: palaeoenvironmental and palaeoclimatic inferences. Quat. Sci. Rev. 180, 177–192. https://doi.org/10.1016/j.quascirev.2017.11.013.

Snyder, C.W., 2016. Evolution of global temperature over the past two million years. Nature 538 (7624), 226–228.

ter Braak, C.J.F., Šmilauer, P., 2018. Canoco reference manual and user's guide: software for ordination (version 5.10). Biometris, Wageningen.

Tinner, W., Lotter, A.F., 2001. Central European vegetation response to abrupt climate change at 8.2 ka. Geology 29 (6), 551. https://doi.org/10.1130/0091-7613(2001)029<0551:CEVRTA>2.0.CO.

Tzedakis, P.C., 1993. Long-term tree populations in northwest Greece through multiple Quaternary climatic cycles. Nature 364 (6436), 437–440. https://doi.org/10.1038/364437a0.

Tzedakis, P.C., 1994. Vegetation change through glacial—interglacial cycles: a long pollen sequence perspective. Phios T R Soc B 345 (1314), 403–432. https://doi.org/10.1098/rstb.1994.0118.

Tzedakis, P.C., Andrieu, V., Beaulieu, J.-L. de, Birks, H.J.B., Crowhurst, S.J., Follieri, M., Hooghiemstra, H., Magri, D., Reille, M., Sadori, L., Shackleton, N.J., Wijmstra, T.A., 2001. Establishing a terrestrial chronological framework as a basis for biostratigraphical comparisons. Quat. Sci. Rev. 20, 1583–1592. https://doi.org/10.1016/S0277-3791(01)00025-7.

Tzedakis, P.C., Andrieu, V., Beaulieu, J.-L. de, Crowhurst, S.J., Follieri, M., Hooghiemstra, H., Magri, D., Reille, M., Sadori, L., Shackleton, N.J., Wijmstra, T.A., 1997. Comparison of terrestrial and marine records of changing climate of the last 500,000 years. Earth Planet Sci. Lett. 150 (1–2), 171–176. https://doi.org/10.1016/s0012-821x(97)00078-2.

Tzedakis, P.C., Crucifix, M., Mitsui, T., Wolff, E.W., 2017. A simple rule to determine which insolation cycles lead to interglacials. Nature 542 (7642), 427.

Tzedakis, P.C., Hodell, D.A., Nehrbass-Ahles, C., Mitsui, T., Wolff, E.W., 2022. Marine isotope stage 11c: an unusual interglacial. Quat. Sci. Rev. 284, 107493 https://doi.org/10.1016/j.quascirev.2022.107493.

Tzedakis, P.C., McManus, J.F., Hooghiemstra, H., Oppo, D.W., Wijmstra, T.A., 2003. Comparison of changes in vegetation in northeast Greece with records of climate variability on orbital and suborbital frequencies over the last 450 000 years. Earth Planet Sci. Lett. 212 (1–2), 197–212. https://doi.org/10.1016/s0012-821x(03)00233-4.

Tzedakis, P.C., Raynaud, D., McManus, J.F., Berger, A., Brovkin, V., Kiefer, T., 2009. Interglacial diversity. Nat. Geosci. 2 (11), 751–755. https://doi.org/10.1038/ngeo660.

Tzedakis, P.C., Roucoux, K.H., Abreu, L. de, Shackleton, N.J., 2004. The duration of forest stages in southern Europe and interglacial climate variability. Science 306 (5705), 2231–2235. https://doi.org/10.1126/science.1102398.

van der Wiel, A.M., Wijmstra, T.A., 1987a. Palynology of the 112.8–197.8 m interval of the core Tenaghi Philippon III, middle Pleistocene of Macedonia. Rev. Palaeobot. Palynol. 52 (2–3), 89–117. https://doi.org/10.1016/0034-6667(87)90048-0.

van der Wiel, A.M., Wijmstra, T.A., 1987b. Palynology of the lower part (78–120 M) of the core Tenaghi Philippon II, middle Pleistocene of Macedonia, Greece. Rev. Palaeobot. Palynol. 52 (2–3), 73–88. https://doi.org/10.1016/0034-6667(87)90047-9.

Wagner, B., Tauber, P., Francke, A., Leicher, N., Binnie, S.A., Cvetkoska, A., Jovanovska, E., Just, J., Lacey, J.H., Levkov, Z., Lindhorst, K., Kouli, K., Krastel, S., Panagiotopoulos, K., Ulfers, A., Zaova, D., Donders, T.H., Grazhdani, A., Koutsodendris, A., Leng, M.J., Sadori, L., Scheinert, M., Vogel, H., Wonik, T., Zanchetta, G., Wilke, T., 2023. The geodynamic and limnological evolution of Balkan Lake Ohrid, possibly the oldest extant lake in Europe. Boreas 52 (1), 1–26. https://doi.org/10.1111/bor.12601.

Wagner, B., Vogel, H., Francke, A., Friedrich, T., Donders, T.H., Lacey, J.H., Leng, M.J., Regattieri, E., Sadori, L., Wilke, T., Zanchetta, G., Albrecht, C., Bertini, A., Combourieu-Nebout, N., Cvetkoska, A., Giaccio, B., Grazhdani, A., Hauffe, T., Holtvoeth, J., Joannin, S., Jovanovska, E., Just, J., Kouli, K., Kousis, I., Koutsodendris, A., Krastel, S., Lagos, M., Leicher, N., Levkov, Z., Lindhorst, K., Masi, A., Melles, M., Mercuri, A.M., Nomade, S., Nowaczyk, N.R., Panagiotopoulos, K., Peyron, O., Reed, J.M., Sagnotti, L., Sinopoli, G., Stelbrink, B., Sulpizio, R., Timmermann, A., Tofilovska, S., Torri, P., Wagner-Cremer, F., Wonik, T., Zhang, X., 2019. Mediterranean winter rainfall in phase with African monsoons during the past 1.36 million years. Nature 573 (7773), 256–260. https://doi.org/10.1038/s41586-019-1529-0.

Wagner, B., Wilke, T., Francke, A., Albrecht, C., Baumgarten, H., Bertini, A., Combourieu-Nebout, N., Cvetkoska, A., D'Addabbo, M., Donders, T.H., Föller, K., Giaccio, B., Grazhdani, A., Hauffe, T., Holtvoeth, J., Joannin, S., Jovanovska, E., Just, J., Kouli, K., Koutsodendris, A., Krastel, S., Lacey, J.H., Leicher, N., Leng, M.J., Levkov, Z., Lindhorst, K., Masi, A., Mercuri, A.M., Nomade, S., Nowaczyk, N.R., Panagiotopoulos, K., Peyron, O., Reed, J.M., Regattieri, E., Sadori, L., Sagnotti, L., Stelbrink, B., Sulpizio, R., Tofilovska, S., Torri, P., Vogel, H., Wagner-Cremer, F., Wolff, G.A., Wonik, T., Zanchetta, G., Zhang, X., 2017. The environmental and evolutionary history of Lake Ohrid (FYROM/Albania): interim results from the SCOPSCO deep drilling project. Biogeosciences 14 (8), 2033–2054. https://doi.org/10.5194/bg-14-2033-2017.

Wijmstra, T.A., 1969. Palynology of the first 30 metres of a 120 m deep section in Northern Greece. Acta Bot. Neerl. 18 (4), 511–527.

Wijmstra, T.A., Smit, A., 1976. Palynology of the middle part (30-78 metres) of the 120 m deep section in Northern Greece (Macedonia). Acta Bot. Neerl. (25), 297–312.

WMO, 2022. World Weather Information Service. https://worldweather.wmo.int/en/city.html?cityId=1499.

Yin, Q.Z., Berger, A., 2012. Individual contribution of insolation and CO2 to the interglacial climates of the past 800,000 years. Clim. Dynam. 38 (3–4), 709–724. https://doi.org/10.1007/s00382-011-1013-5.

Yin, Q.Z., Berger, A., 2015. Interglacial analogues of the Holocene and its natural near future. Quat. Sci. Rev. 120, 28–46. https://doi.org/10.1016/j.quascirev.2015.04.008.

Zanchetta, G., Regattieri, E., Giaccio, B., Wagner, B., Sulpizio, R., Francke, A., Vogel, H., Sadori, L., Masi, A., Sinopoli, G., Lacey, J.H., Leng, M.J., Leicher, N., 2016. Aligning and synchronization of MIS5 proxy records from Lake Ohrid (FYROM) with independently dated Mediterranean archives: implications for DEEP core chronology. Biogeosciences 13 (9), 2757–2768. https://doi.org/10.5194/bg-13-2757-2016.

Zolitschka, B., Rolf, C., Bittmann, F., Binot, F., Frechen, M., Wonik, T., Froitzheim, N., Ohlendorf, C., 2014. Pleistocene climatic and environmental variations inferred from a terrestrial sediment record–the Rodderberg Volcanic Complex near Bonn, Germany. Z. Dtsch. Ges. Geowiss. 165 (3), 407–424.